doi:10.1111/evo.13377

Host conservatism, geography, and elevation in the evolution of a Neotropical moth radiation

Joshua P. Jahner,[1,2] Matthew L. Forister,[1] Thomas L. Parchman,[1] Angela M. Smilanich,[1] James S. Miller,[3] Joseph S. Wilson,[4] Thomas R. Walla,[5,6] Eric J. Tepe,[7] Lora A. Richards,[1] Mario Alberto Quijano-Abril,[8] Andrea E. Glassmire,[1] and Lee A. Dyer[1,6]

[1]*Program in Ecology, Evolution, and Conservation Biology, Department of Biology, University of Nevada, Reno, Nevada 89557*

[2]*E-mail: jpjahner@gmail.com*

[3]*Division of Invertebrate Zoology, American Museum of Natural History, New York, New York 10024*

[4]*Department of Biology, Utah State University, Tooele, Utah 84074*

[5]*Department of Biology, Colorado Mesa University, Grand Junction, Colorado 81507*

[6]*Seccion Invertebrados, Museo Ecuatoriano de Ciencias Naturales, Quito, Ecuador*

[7]*Department of Biological Sciences, University of Cincinnati, Cincinnati, Ohio 45221*

[8]*Grupo de Estudios Florísticos, Herbario Universidad Católica de Oriente, Rionegro, Antioquia, Colombia*

Received April 20, 2017
Accepted September 20, 2017

The origins of evolutionary radiations are often traced to the colonization of novel adaptive zones, including unoccupied habitats or unutilized resources. For herbivorous insects, the predominant mechanism of diversification is typically assumed to be a shift onto a novel lineage of host plants. However, other drivers of diversification are important in shaping evolutionary history, especially for groups residing in regions with complex geological histories. We evaluated the contributions of shifts in host plant clade, bioregion, and elevation to diversification in *Eois* (Lepidoptera: Geometridae), a hyper-diverse genus of moths found throughout the Neotropics. Relationships among 107 taxa were reconstructed using one mitochondrial and two nuclear genes. In addition, we used a genotyping-by-sequencing approach to generate 4641 SNPs for 137 taxa. Both datasets yielded similar phylogenetic histories, with relationships structured by host plant clade, bioregion, and elevation. While diversification of basal lineages often coincided with host clade shifts, more recent speciation events were more typically associated with shifts across bioregions or elevational gradients. Overall, patterns of diversification in *Eois* are consistent with the perspective that shifts across multiple adaptive zones synergistically drive diversification in hyper-diverse lineages.

KEY WORDS: **Andes Mountains, Central American Seaway, ecological opportunity, *Eois*, genotyping-by-sequencing, *Piper*.**

Adaptive radiations illustrate the potential for ecological processes to shape long-term evolutionary dynamics (Simpson 1953; Schluter 2000). They are characterized by the rapid diversification of ecologically differentiated species, occasionally resulting in convergent evolution of similar forms across distantly related lineages (Muschick et al. 2012; Mahler et al. 2013; Wilson et al. 2015; Esquerré and Keogh 2016). Adaptive radiations are facilitated by ecological opportunity associated with the invasion of novel adaptive zones (Simpson 1953; Losos 2010; Yoder et al. 2010; Stroud and Losos 2016), often via dispersal into previously unoccupied habitats or onto an island with open niche space (Lack 1947; Carlquist 1974; Lerner et al. 2011; Haines et al. 2014). Similarly, ecological opportunity can arise from the development of a key evolutionary innovation that allows for the colonization of a previously unutilized resource type (e.g., Hodges and Arnold 1995; Martin and Wainwright 2011; Matschiner et al. 2011). For

example, North American crossbills (Fringillidae: genus *Loxia*) have evolved crossed mandibles that are an evolutionary innovation for opening the cones of conifers, and specialization on different cone morphologies has led to rapid diversification (Benkman 1993; Benkman et al. 2010).

While the role of ecological opportunity in stimulating diversification has been characterized for many adaptive radiations, few studies have attempted to compare the roles of multiple potential adaptive zones concurrently within the same evolutionary context (e.g., Givnish et al. 2009; Mahler et al. 2013; Lagomarsino et al. 2016), perhaps because it can be difficult to disentangle ecological opportunity from simple isolation (e.g., geography, elevation, etc.). In herbivorous insects, host plant lineages are thought to be the predominant axis for promoting diversification (Mitter et al. 1988; Fordyce 2010), which has led to hypotheses for explaining the extreme diversity of phytophagous insects and the plants they feed upon (Ehrlich and Raven 1964; reviewed by Janz 2011). One of the central patterns that led to the formulation of the escape and radiate hypothesis, which posits that insect lineages often diversify on novel lineages of host plants after developing physiological innovations to mitigate plant defenses (e.g., Wheat et al. 2007; Edger et al. 2015), is that groups of closely related herbivores typically consume closely related host plants (i.e., host conservatism; Ehrlich and Raven 1964). Despite widespread evidence for host conservatism in herbivorous insect radiations (Winkler and Mitter 2008), few studies have explicitly examined the relative importance of host lineages as adaptive zones versus more straightforward geographic differentiation (e.g., Becerra 1999; Condamine et al. 2012; Calatayud et al. 2016).

The moth genus *Eois* (Lepidoptera: Geometridae, Larentiinae) is an ideal system for investigating the effects of host conservatism and geography on diversification. More than 250 *Eois* species have been formally described, 83% of which are restricted to the New World; however, the true diversity of the genus is estimated at more than 1000 species in the Neotropics alone (Brehm et al. 2011). *Eois* caterpillars are highly specialized feeders, with each species typically feeding on only one or two host species (Connahs et al. 2009) within the diverse genus *Piper* (Piperaceae), although rare host associations have also been documented with plants in other genera (Strutzenberger et al. 2010; Seifert et al. 2015). Roughly 1300 *Piper* species occur in the Neotropics (~70% of global species diversity; Martínez et al. 2015), providing ample opportunity for host-associated diversification in *Eois*. Previous molecular investigations of *Eois* have reported strong host conservatism, with lineages of related caterpillars specializing on closely related host plants (Strutzenberger et al. 2010; Wilson et al. 2012). Elevational differences, especially associated with the Andes Mountains, are also thought to promote *Eois* diversification (Strutzenberger and Fiedler 2011; Glassmire et al. 2016), resulting in elevationally stratified *Eois* communities (Rodríguez-Castañeda et al. 2010). Overall, two of the most important documented drivers of diversification in *Eois* are the Andean uplift and the diversification of *Piper*, both of which occurred during the Miocene, the geological period associated with the highest rates of *Eois* diversification (Strutzenberger and Fiedler 2011; Martínez et al. 2015).

Previous molecular analyses of *Eois* (Strutzenberger et al. 2010; Wilson et al. 2012) have focused almost exclusively on species found at three collection localities—Southern Ecuador, Central Ecuador, and Costa Rica—even though *Eois* occurs throughout the Neotropics from southern Mexico to northern Argentina (Brehm et al. 2011). The full distributional range of this genus spans regions that were dramatically affected by complex geological change over the past 50 million years, including the rise of the Andes (Hoorn et al. 2010) and the closure of the Central American Seaway that once separated North and South America (Montes et al. 2015). These geological events have been implicated in the phylogeographic histories of numerous organisms from a variety of taxonomic groups (Daza et al. 2010; Hoorn et al. 2010; Turchetto-Zolet et al. 2013; Bagley and Johnson 2014; Bacon et al. 2015) and have likely impacted the evolutionary history of *Eois* as well. More specifically, the colonization of novel bioregions and elevational bands by different *Eois* lineages could allow for rapid diversification through nonmutually exclusive processes: (1) allopatric isolation and (2) effects of ecological opportunity following the colonization of new adaptive zones (e.g., novel habitat types or host species).

Here, we examine phylogenetic relationships among *Eois* species sampled from a far wider geographic range than in previous studies to investigate the roles of host conservatism, geography, and elevation in structuring patterns of diversification. Specifically, we test the following hypotheses: (1) associations with host plant clades will show relatively greater conservatism, associated with earlier radiations in *Eois*, while shifts in geography and elevation will be more frequent, and more frequently linked to recent speciation events; and (2) overall rates of diversification will be elevated in association with the colonization of novel host clades, geographic regions, and elevational bands. Given extensive documented support for the colonization of novel host lineages in facilitating insect diversification, we expected that the most elevated rates would be associated with host clades, followed by both bioregions and elevation.

Materials and Methods

SPECIMEN COLLECTION

Eois caterpillars and adults were collected from sites in eight Central and South American countries or dependencies (Fig. 1; Table S1), including two sites previously examined by Wilson et al. (2012): Yanayacu Biological Station in Ecuador and La Selva

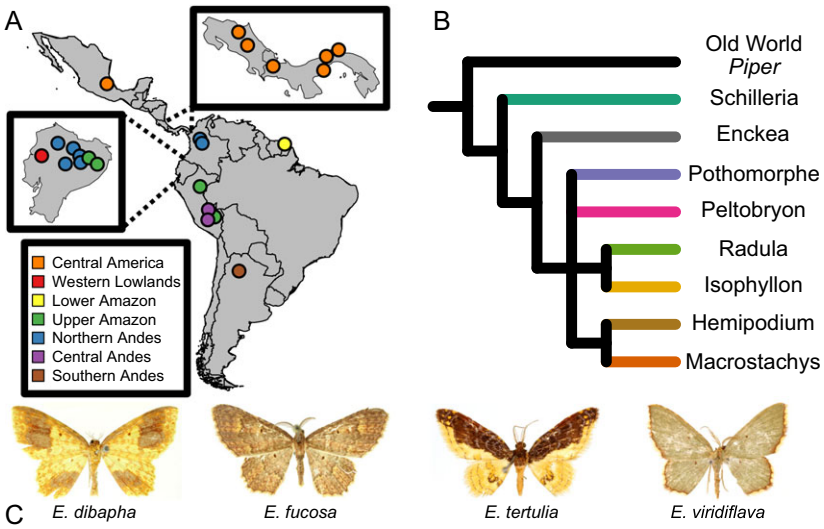

Figure 1. ***Eois*** **caterpillars and moths were collected from multiple locations (A) encompassing eight countries across the Neotropics, including individuals feeding on nearly all of the New World** ***Piper*** **clades (B) (topology from Jaramillo et al. 2008; see main text for details about differences among** ***Piper*** **clades; Table S1). Each dot on the map represents a different sampling locality, which was categorized into one of seven bioregions roughly based on the designations of Chazot et al. (2016). The colors on the map and the** ***Piper*** **topology match those found in Figures 2 and 3. (C) Dorsal views of four** ***Eois*** **species included in the study.**

Biological Station in Costa Rica. Sampling sites were selected to maximize the geographic range, elevational span, and host plant diversity of *Eois*. Specimens were collected via one of three methods: plot-based larval collecting, general larval collecting, or light trapping of adults. Plot-based collection involved searching for caterpillars on all *Piper* leaves in 5–30 m diameter plots for a standardized amount of time, ranging from 1–3 hours (e.g., Dyer et al. 2010; Rodríguez-Castañeda et al. 2010) and is typically utilized at permanent sites to standardize sampling effort when comparing ecological data across sites (Dyer et al. 2007; Forister et al. 2015). In contrast, general collection involved walking on trails, haphazardly through the forest, or along transects while searching all encountered *Piper* plants for caterpillars.

Caterpillars were either immediately preserved in ethanol or were reared using standard protocols (Gentry and Dyer 2002) to collect emerging adults of moths or parasitoid flies and wasps for ecological data and taxonomic identification. *Eois* specimens were deposited in: University of Nevada, Reno, Museum of Natural History Entomology Research Collection (UNR-ENTO), United States National Museum of Natural History (USNM), and Museo Ecuatoriano de Ciencias Naturales (MECN). Host plant specimens were also collected for identification and assignment to host plant clade (sections, or informal groupings) following Jaramillo et al. (2008; Fig. 1; Table S1). We were unable to assign a host plant designation to adult moths collected via light trapping (Table S1). Vouchers for Colombian host plants were identified by MAQA and deposited in the Herbario Universidad Católica de Oriente (HUCO). All other host plant vouchers were identified by EJT and deposited in: Margaret H. Fulford Herbarium, University of Cincinnati (CINC), Herbario Nacional, Museo Nacional de Costa Rica (CR), Missouri Botanical Garden (MO), W.S. Turrell Herbarium, Miami University (MU), Herbario, Universidad de Panamá (PMA), Herbario, Pontificia Universidad de Católica del Ecuador (QCA), Herbario Nacional del Ecuador (QCNE), and Herbario, Universidad Nacional Mayor de San Marcos, Perú (USM).

Major Neotropical *Piper* clades are thought to have diverged from one another ~50–75 million years ago (Martinez et al. 2015), so these lineages represent phylogenetically distant assemblages of ecologically diverse species (Fig. 1). In this study, we examined host conservatism at the clade level instead of the species level because (1) we do not have genetic data for every host species, and (2) we were focused on broad scale patterns of evolution associated with the utilization of host lineages (*sensu* Ehrlich and Raven 1964). It is worth noting that this approach deemphasizes the strength of speciation facilitated by host shifts within a host plant clade (Wilson et al. 2012) while magnifying the influence of host conservatism.

We were unable to exclusively use nominal taxonomy as a guide for the removal of duplicate samples from subsequent phylogenetic analyses because many of our samples were collected as caterpillars, which cannot always be identified to species at the larval stage (Wilson et al. 2012). Furthermore, cryptic species diversity has been reported in a number of tropical Lepidoptera lineages (e.g., Hebert et al. 2004; Burns et al. 2008; Janzen et al. 2009; Brehm et al. 2016), including *Eois* (Strutzenberger et al. 2011),

so similarities or differences in nominal taxonomy may not be representative of genetic differentiation. Therefore, we took a conservative approach and only included individuals in phylogenetic reconstructions if they were different from one another in at least one of the following aspects: collection locality, host plant, morphology (larval or adult), or DNA sequence (almost all individuals differed in multiple categories). Although this strategy might bias our results toward the discovery of trait conservatism among a small subset of individuals, it should not be biased toward an association between any particular trait state and diversification rates across lineages.

SANGER SEQUENCING

Eois DNA was extracted using Qiagen DNeasy Blood and Tissue kits (Qiagen Inc., Germantown, MD) and quantified using spectrophotometry. One mitochondrial gene (cytochrome *c* oxidase subunit I, COI) and two nuclear genes (elongation factor 1-alpha, EF1-α; wingless, WG) were amplified using PCR (see Table S2 for PCR primers and Table S3 for PCR protocols). Successfully amplified PCR products were cleaned with a Qiagen size exclusion membrane and sequenced using an ABI3730 DNA Analyzer (Applied Biosystems Inc., Foster City, CA) at the Nevada Genomics Center (Reno, NV). Sequences were visually inspected and aligned in Sequencher 4.10.1 (Gene Codes Corp, Ann Arbor, MI).

Phylogenetic trees were first constructed for all three genes individually using Bayesian inference implemented in MrBayes 3.2.3 (Ronquist et al. 2012). Models of evolution were selected by comparing AIC likelihood scores in jModeltest 2.1.5 (Darriba et al. 2012; Arenas 2015) for those models available in MrBayes. The GTR+I+G model of evolution was implemented for phylogenies constructed from nuclear genes (EF1-α and WG), while the HKY+I+G model of evolution was selected for constructing the mitochondrial genealogy (COI). In addition to single gene trees, a phylogeny was generated with all genes concatenated using a GTR+I+G model of evolution. To root each tree, three outgroup species from the subfamily Larentiinae were selected based on a phylogenetic analysis of the family Geometridae (Sihvonen et al. 2011): *Asthena albulata*, *Operophtera brumata*, and *Poecilasthena pulchraria*. All MrBayes analyses were run on the Ohio Supercomputer Center (Ohio Supercomputer Center 1987) using four chains (three heated and one cold) for 5,000,000 Markov chain Monte Carlo (MCMC) iterations. Chains were sampled every 2500 MCMC iterations and a 25% burn-in was employed.

GENOTYPING-BY-SEQUENCING

As a complementary approach to traditional Sanger sequencing, we also constructed reduced-representation genomic libraries for Illumina sequencing using a genotyping-by-sequencing (GBS) approach, which is a form of ddRADseq (Peterson et al. 2012; Parchman et al. 2012). DNA from the extractions described above was cut at restriction recognition sites throughout the genome using two enzymes, EcoRI and MseI. Each *Eois* specimen was assigned a unique 8–10 base pair barcode to allow for highly multiplexed sequencing. Each DNA fragment was ligated to two adaptors: (1) an EcoRI adaptor containing the Illumina adaptor, the individual's unique barcode, and bases matching the restriction enzyme cut site; and (2) an MseI adaptor containing bases matching the cut site and the opposite Illumina adaptor. DNA libraries were amplified using PCR and fragments ranging from 350–450 bases in length were size selected using a Pippin Prep quantitative electrophoresis unit (Sage Science, Beverly, MA). Libraries were sequenced on two lanes of an Illumina HiSeq 2500 at the University of Texas Genomic Sequencing and Analysis Facility (Austin, TX).

Contaminant DNA (PhiX, *E. coli*), low quality fragments, and reads representing Illumina adaptors were filtered from the raw data using Bowtie 2_db (Langmead and Salzberg 2012) along with a set of bash and Perl scripts designed for cleaning contaminants from Illumina data (details on this pipeline can be found at https://github.com/ncgr/tapioca). We used a Perl script to correct single-base errors in barcode identifiers, to associate sample IDs with unique identifiers, and to remove barcode sequences and fragments containing segments of Illumina adaptors.

We used the ipyrad v0.7.1 pipeline (http://github.com/dereneaton/ipyrad; Eaton 2014) for de novo assembly of reads, variant calling, and quality filtering. A number of bioinformatic pipelines now exist for the efficient processing of large GBS or RADseq datasets. Most of these pipelines share many similarities and even utilize the same tools for certain steps, but each pipeline also has a unique set of advantages and disadvantages. We chose to use ipyrad because it performs well with phylogenetic datasets, conducts de novo assemblies, incorporates indel variation, and exports data in several formats that are commonly used as input for phylogenetic analyses (e.g., nexus, phylip) (Eaton 2014). It is worth noting that we explored the outcomes of genotype calling using two alternative bioinformatic pipelines (ipyrad and dDocent (Puritz et al. 2014)), as well as using genotype likelihoods (Li et al. 2009). The SNP datasets from all three approaches yielded phylogenetic trees that were largely concordant with one another, suggesting that our results are relatively robust to the bioinformatic approach employed.

For each of the seven steps in the ipyrad pipeline, default parameters were specified unless otherwise noted. First, demultiplexed FASTQ files for each individual were input into ipyrad, with the data type specified as ddrad. Individual reads were filtered based on quality scores, with the maximum number of Ns in a read (max_low_qual_bases) set to 7. Remaining reads were

dereplicated and then de novo clustered within individual samples with VSEARCH (Rognes et al. 2016) using a minimum sequence similarity threshold (clust_threshold) of 0.80. Clustered sequences were then aligned with MUSCLE (Edgar 2004), resulting in a separate set of alignments for each individual. Rates of heterozygosity and sequencing error were then estimated across sites for subsequent base calling. A binomial model was used for consensus base calling at variable sites if the sequencing depth was greater than or equal to five (mindepth_statistical). Alternatively, majority rule base calls were performed if the sequencing depth was less than five but greater than or equal to two (mindepth_majrule). Additionally, the maximum number of Ns per locus (max_Ns_consens) and maximum number of heterozygous bases per locus (max_Hs_consens) was set to 10 for base calling. Sequences were then clustered across individual samples and aligned as described above, resulting in one set of alignments for the entire dataset. The final alignments were then quality filtered, with the minimum number of individuals that must have data at a locus (min_samples_locus) set to 70%, the maximum number of snps at a locus (max_snps_locus) set to 30, and the maximum number of indels per locus (max_Indels_locus) set to 10. After filtering, the final dataset was exported as concatenated sequences in PHYLIP format.

An approximately maximum-likelihood tree was constructed in FastTree 2.1.9 (Price et al. 2010). Several issues can arise by constructing phylogenetic trees using concatenated SNPs instead of using alternative species tree approaches (Liu et al. 2015; Leaché and Oaks 2017). However, these issues can be partially ameliorated by using concatenated sequences that also contain invariant sites (Leaché et al. 2015a), which we did here. We first used a custom Perl script to convert the PHYLIP file exported from ipyrad into a FASTA file for use with FastTree. Because we utilized concatenated sequences in the FASTA input file, the GTR + CAT model of evolution was specified for tree construction. Local support values for each node in the phylogeny were calculated using Shimodaira-Hasegawa tests (Shimodaira and Hasegawa 1999). The final tree was rooted with the most basal *Eois* group from the Sanger tree (group "A," see below).

TRAIT EVOLUTION

All analyses of trait evolution were conducted using both the concatenated Sanger and GBS phylogenies. We first employed maximum likelihood to reconstruct ancestral character states for three discrete traits (Pagel 1994): host plant clade, bioregion, and elevational band. Sample sites were categorized into one of seven bioregions loosely based on the designations of Chazot et al. (2016): Central America, Western Lowlands, Lower Amazon, Upper Amazon, Northern Andes, Central Andes, and Southern Andes (see Fig. 1). Similarly, elevation was categorized based on previously delineated elevational bands that roughly correspond to different forest types (Rodríguez-Castañeda et al. 2010): <1000 m (lowland rainforest); 1000–1700 m (montane forest); 1700–3000 m (upper montane forest; Table S1; Figs. S1 and S2). All three reconstructions were performed using the "ace" function of the ape package (Paradis et al. 2004) in R (R Core Team 2015). We tested six alternative models of evolution for the elevation ancestral trait reconstruction and chose the model with the lowest AIC value (see Tables S4 and S5 for more details). An equal rates model of evolution was specified for the host plant clade and bioregion reconstructions due to the large number of alternative states for these traits.

In addition, we tested whether host plant clade, bioregion, and elevation (as a categorical trait) were clustered nonrandomly across the trees using three complementary analyses in the Bayesian Tip-Association Significance Testing (BaTS) software (Parker et al. 2008): parsimony score (PS; Slatkin and Maddison 1989), association index (AI; Wang et al. 2001), and maximum monophyletic clade size (MC; Parker et al. 2008). While PS and AI calculate a degree of phylogenetic clustering across all trait states across a phylogeny, MC is a measure of clustering for each alternative trait state (e.g., Northern Andes for an analysis of bioregion; see Parker et al. 2008 for a detailed review of all three metrics). To test the null hypothesis that traits (PS and AI) and alternative trait states (MC) are randomly distributed across the phylogeny, observed values were compared to estimates from 1000 permutations of traits randomly shuffled across the phylogeny.

To test whether closely related *Eois* specimens share similar elevational distributions as a continuous trait, we estimated two complementary metrics of phylogenetic signal, Pagel's λ (Pagel 1999) and K (Blomberg et al. 2003), using the "phylosig" function of the phytools package (Revell 2012) in R. Phylogenetic signal refers to the tendency of closely related individuals to share more similar trait values as compared to more distant relatives (Blomberg and Garland 2002; reviewed by Kamilar and Cooper 2013). Values of Pagel's λ, a measure of the covariance among traits with respect to phylogenetic signal, range from 0 to 1 (no signal to strong signal, respectively; Pagel 1999). K is calculated as the ratio of observed phylogenetic signal versus the expected signal under a model of Brownian motion, with values ranging from 0 to ∞ (Blomberg et al. 2003). $K = 1$ indicates that a trait has evolved under a model of Brownian motion (strong phylogenetic signal), $K < 1$ represents weak or absent signal, and $K > 1$ implies that closely related individuals have more similar trait values than expected. We tested whether estimates of Pagel's λ were significantly greater than zero using a log-likelihood test comparing the likelihood of the observed estimate to that of a tree constrained to have Pagel's $\lambda = 0$. Significance for K was inferred with a permutation approach.

RATES OF DIVERSIFICATION

We first asked how often shifts among bioregions, host plant clades, and elevational distributions (as categorical traits) were associated with speciation events using the Cladogenetic State Speciation and Extinction (ClaSSE; Goldberg and Igic 2012) method as implemented in the diversitree package (FitzJohn 2012) in R. ClaSSE models allow for the estimation of three types of speciation rates for multiple traits simultaneously. Anagenetic rates (q) are associated with one trait changing into another trait without a branching event along a tree (e.g., q_{L-M} = a species shift from low elevation to mid elevation without a divergence event). Alternatively, cladogenetic speciation rates (λ) are always associated with a divergence event, and can include shifts to derived traits (e.g., $\lambda_{L<L,M}$ = a low elevation ancestor diverging into low and mid elevation descendants) or divergence without trait shifts (e.g., $\lambda_{L<L,L}$ = a low elevation ancestor diverging into two low elevation descendants). Additionally, ClaSSE models also estimate extinction rates (μ) for each alternative trait state (e.g., μ_L = the extinction rate for low elevation taxa).

Due to the large number of parameters included in ClaSSE models with numerous alternative trait states, we constrained several parameters to equal zero in all models following Chazot et al. (2016). Specifically, we constrained all cladogenetic rates (λ) where both descendants had a different trait state than the ancestor (e.g., $\lambda_{L<M,H}$) and all anagenetic rates (q) to equal zero. For the host plant clade ClaSSE, individuals consuming species of the Isophyllon ($N = 1$) or Hemipodium ($N = 2$) clades were grouped with individuals feeding on closely related host plant clades (Radula and Macrostachys, respectively; Fig. 1). The sole individual feeding on Enckea was treated as unknown for this analysis due to the lack of a closely related host plant clade (Fig. 1; Table S1). We implemented maximum likelihood using the *find.mle* function (maxit = 100,000) to evaluate 32 alternative models for the bioregion ClaSSE, 24 models for the elevation ClaSSE, and 12 models for the host plant clade ClaSSE (see Tables S6, S7, and S8 for more details about each alternative model). Parameters from the top model of each ClaSSE analysis (based on Δ AIC) were subsequently estimated across 10,000 MCMC iterations using the *mcmc* function. To assess whether parameters were significantly different from one another (within each of the three ClaSSE models), pairwise joint probabilities (P_J) were calculated to determine if posterior distributions were significantly different from one another. P_J is the number of parameter steps in which one parameter is larger than the other parameter, and significance was assessed at $\alpha = 0.05$.

Finally, we used Bayesian Analysis of Macroevolutionary Mixtures (BAMM) (Rabosky 2014) to ask if and how rates of diversification vary across the *Eois* GBS phylogeny. BAMM implements a reversible jump MCMC to explore potential diversification rate heterogeneity across lineages of a phylogeny, allowing for the identification of unique macroevolutionary regimes that occur within a phylogeny without a priori information. The "setBAMMpriors" function in the BAMMtools package (Rabosky et al. 2014) in R was used to estimate starting values for the expectedNumberOfShifts, lambdaInitPrior, lambdaShiftPrior, and muInitPrior priors. Default values were specified for all other parameters. A speciation-extinction model was run for 100 million MCMC generations, sampling every 20,000 generations with a 10% burnin. Parameter convergence was inspected visually in R.

Results

TRAIT EVOLUTION – SANGER SEQUENCING

For 107 *Eois* individuals, we sequenced 617 base pairs (bp), 679bp, and 463bp of COI, EF1-α, and WG, respectively. For all four of the phylogenetic trees constructed with MrBayes (COI, EF1-α, WG, concatenated), the minimum ESS was much greater than 200 and the PRSF approached 1.0. The single gene trees were unable to fully resolve the phylogenetic history of *Eois*, especially along the backbone (Fig. S3). Of the three gene trees, COI provided the least phylogenetic resolution and yielded almost no information regarding backbone structure, while the nuclear gene trees (EF1-α and WG) provided deeper resolution (Fig. S3). All three trees have apparent polytomies, with the groups labeled "A" and "B" basal for COI and EF1-α, but not for WG. In general, the "C," "D," "E," "F," and "G" groups were composed of roughly the same individuals across the three gene trees, but the relative positions of these groups were unresolved due to the large polytomies.

Concatenation of the three genes produced a tree in which most nodes were resolved (Fig. 2). An exploration of how alternative partitioning schemes affected tree topology using PartitionFinder2 (Lanfear et al. 2017) resulted in trees with very similar topologies, with all differences occurring at nodes with low support (data available upon request). Across the concatenated tree, *Eois* individuals were clustered strongly by bioregion, elevation, and host plant clade (Figs. 2, S4, S5). This qualitative assessment was confirmed by the estimates of association index (AI) and parsimony score (PS): all three traits were significantly clustered on the phylogeny for both metrics (Table 1). For alternative trait states, the MC (monophyletic clade size) analysis revealed that all bioregion and host clade alternative states were significantly clustered on the concatenated tree except for individuals found in the lower Amazon ($N = 5$; $P = 0.056$) and the Isophyllon clade of host plants ($N = 2$; $P = 1$; Table 2). In contrast, only low elevation individuals (< 1000 m) were significantly clustered on the concatenated tree. Finally, estimates of phylogenetic signal for the elevational distribution of *Eois* were significantly greater than zero for both estimates (Pagel's $\lambda = 1.000$; $P < 0.001$; $K = 0.176$; $P = 0.001$).

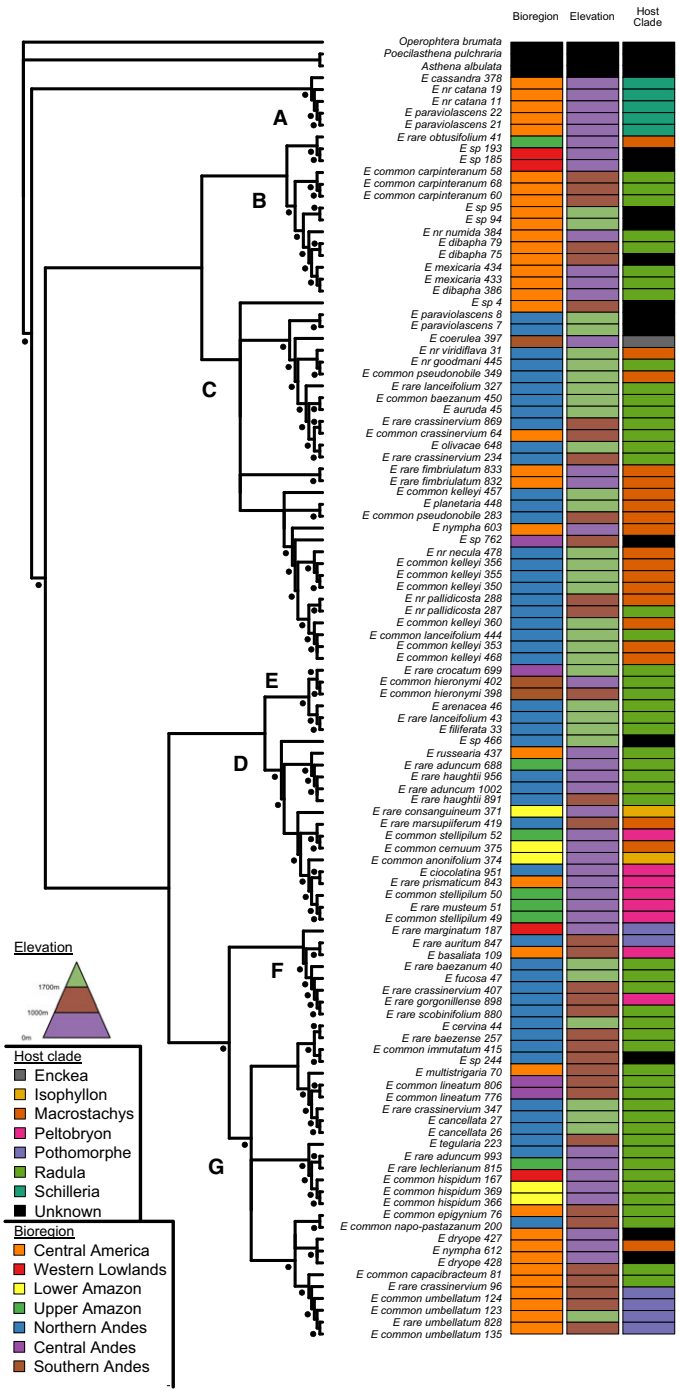

Figure 2. The distribution of bioregion, elevational, and host plant clade variation is displayed across the concatenated Sanger tree (COI, EF1-α, WG). Individuals not identified to species are labeled as either rare or common (depending on how many individuals were collected), followed by the host plant species name. From left to right, the bars on the right of the figure display current tip states for bioregion, elevation, and host plant clade. Individuals without known host plant clade designations are colored black. Additional individual collection data can be found in Table S1. Groups of related *Eois* are labeled "A" – "G" for easy reference in the main text. Nodes with strong support (posterior probability of at least 0.90) are denoted with a black circle.

Table 1. Observed association indices (AI; Wang et al. 2001) and parsimony scores (PS; Slatkin and Maddison 1989); measurements of trait clustering were compared to expected values from 1000 tree-tip shuffling permutations to test the null hypothesis that traits were randomly distributed across phylogenies.

Dataset	Trait	Analysis	Observed	Expected Mean (95% CI)
Sanger	Bioregion	AI	2.18	7.90 (6.73 – 9.01)
		PS	28	48.81 (45 – 53)
	Elevation	AI	2.02	7.79 (6.55 – 9.03)
		PS	27	49.82 (45 – 54)
	Host clade	AI	2.43	8.18 (7.05 – 9.20)
		PS	26	50.02 (46 – 53)
GBS	Bioregion	AI	2.17	11.30 (9.93 – 12.64)
		PS	34	67.29 (63 – 72)
	Elevation	AI	3.69	10.53 (8.99 – 12.04)
		PS	34	63.83 (59 – 69)
	Host clade	AI	3.72	11.17 (9.82 – 12.37)
		PS	36	63.72 (60 – 67)

Both analyses were conducted on bioregion, elevation, and host plant clade using both datasets (GBS and Sanger sequencing). Significant clustering was inferred if $P < 0.05$, and all values were significant for all analyses ($P < 0.001$).

TRAIT EVOLUTION – GENOTYPING-BY-SEQUENCING

After initial filtering and contaminant removal, 255,133,183 sequences from 137 individuals (mean = 1,862,286) were used for analysis with ipyrad. The final assembly output from ipyrad was 18,376 bp long and consisted of 4641 SNPs spanning 201 contigs, with an average of 23.1 SNPs per contig (sd = 5.73). On average, individuals were missing 20.2% of data (sd = 5.34%). Not surprisingly, the maximum-likelihood tree (Figs. 3, S6) yielded a similar phylogenetic history as the concatenated tree from Sanger sequencing (Fig. 2). The individuals included in both datasets were found in the same groups ("A" – "G"), though the relative positions of these groups varied slightly in the two trees (Figs. 2, 3). For instance, group "B" was placed sister to group "C" in the Sanger tree with low support (Fig. 2), but was placed in a more basal position in the GBS tree with strong support (Figs. 3, S6). Additionally, groups "D" and "E" were grouped together and placed sister to groups "F" and "G" in the Sanger tree with low support (Fig. 2), while the GBS tree yielded a topology with group "E" sister to groups "F" and "G" (with low support), and group "D" sister to groups "E," "F," and "G" (with strong support; Figs. 3, S6). Despite inconsistencies between trees, which can largely be attributed to poorly supported nodes in the Sanger dataset, the two trees are strongly concordant considering the two different methodologies employed.

As in the concatenated Sanger tree, *Eois* taxa were strongly clustered by bioregion, elevation, and host plant clade across the GBS tree (Figs. 3 and S7), as supported by both the AI and PS metric (Table 1). All bioregions in the MC analysis were significantly clustered on the GBS tree except taxa found in the western lowlands ($N = 7$; $P = 0.109$) (Table 2). Additionally, all host plant clades were significantly grouped except Pothomorphe ($N = 8$; $P = 0.134$), while only the high elevation individuals displayed nonsignificant clustering in the elevation MC analysis ($N = 36$; $P = 0.319$) (Table 2). Estimates of elevational phylogenetic signal for the GBS tree (Pagel's $\lambda = 0.931$; $P < 0.001$; $K = 0.093$; $P = 0.001$) were similar in magnitude to estimates from the concatenated Sanger tree.

RATES OF DIVERSIFICATION

For the bioregion ClaSSE analysis, we first fit 32 alternative models using maximum likelihood to select the top model using AIC (Table S6). Model selection clearly favored a model with only two bioregion classes (Andean vs non-Andean), as opposed to models with either three bioregions (Andean, Amazonian, and Central America/Western Lowlands) or all seven of the bioregions depicted in Fig. 1 (Table S6). Of the six models with Δ AIC < 2, half of the models did not allow all speciation rates (λ) associated with a state change to differ (including the top model), while the other three models did allow variation. The top model that was subsequently fit with MCMC included one extinction parameter that was equal for both Andean (A) and non-Andean (N) lineages (i.e., $\mu_A = \mu_N$), one speciation parameter associated with trait shifts (λ shift), and another speciation parameter not associated with trait shifts (λ no shift). λ shift (median = 2.91; 95% CI: 1.54–5.13; Fig. 4) was significantly smaller than λ no shift (median = 39.51; 95% CI = 30.35–52.90) ($P_J < 0.001$; Fig. 4; Table S10). Also, the extinction rate (μ; median = 41.70; 95%

Table 2. Results from the maximum monophyletic clade (MC) size analyses (Parker et al. 2008), which tested the null hypothesis that alternative states for bioregion, host plant clade (genus *Piper*), and elevation were distributed randomly across the *Eois* phylogeny.

Dataset	Trait	Alternative state	*N*	Observed MC	Null MC	*P*
Sanger	Bioregion	Central America	35	11	2.53	**< 0.001**
		Western Lowlands	4	2	1.03	**0.030**
		Lower Amazon	5	2	1.06	0.056
		Upper Amazon	7	3	1.12	**0.006**
		Northern Andes	49	10	3.36	**0.002**
		Central Andes	4	2	1.03	**0.030**
		Southern Andes	3	2	1.02	**0.018**
	Elevation	Low	39	6	2.76	**0.018**
		Medium	35	3	2.54	0.449
		High	33	4	2.42	0.066
	Host clade	Isophyllon	2	1	1.00	1.000
		Macrostachys	20	4	1.78	**0.008**
		Peltobryon	8	5	1.15	**< 0.001**
		Pothomorphe	6	4	1.08	**< 0.001**
		Radula	52	7	3.56	**0.008**
		Schilleria	5	5	1.06	**< 0.001**
GBS	Bioregion	Central America	48	6	2.87	**0.014**
		Western Lowlands	7	2	1.11	0.109
		Lower Amazon	4	2	1.02	**0.025**
		Upper Amazon	11	4	1.23	**< 0.001**
		Northern Andes	55	8	3.20	**0.005**
		Central Andes	9	3	1.15	**0.004**
		Southern Andes	3	2	1.02	**0.017**
	Elevation	Low	53	10	3.07	**< 0.001**
		Medium	48	9	2.89	**0.002**
		High	36	3	2.35	0.319
	Host clade	Hemipodium	2	2	1.00	**0.005**
		Macrostachys	23	4	1.83	**0.006**
		Peltobryon	10	7	1.21	**< 0.001**
		Pothomorphe	8	2	1.14	0.134
		Radula	69	9	4.01	**0.008**
		Schilleria	6	6	1.07	**< 0.001**

A separate analysis was run for each trait, in which the observed MC was compared to a null MC from 1000 tree randomizations for each alternative state. Significant clustering of traits (denoted by bold text) was inferred for alternative states that rejected the null hypothesis ($P < 0.05$). Both analyses were performed using phylogenies created from the GBS and Sanger sequencing (concatenated tree) datasets. The results from alternative states that were comprised of a single individual are not reported (GBS/Host Clade: Enckea, Isophyllon; Sanger/Host Clade: Enckea).

CI = 41.70–55.87) was significantly larger than λ shift but not λ no shift (Table S10).

Twenty-four alternative models were fit with maximum likelihood for the elevation ClaSSE analysis (Table S7). Two of the three models with Δ AIC < 2 allowed speciation rates associated with state changes to vary symmetrically (e.g., $\lambda_{L<L,M} = \lambda_{M<M,L}$), and all three top models included speciation rates with shifts between low and high elevations (i.e., $\lambda_{L<L,H}$ and $\lambda_{H<H,L} \neq 0$) (Table S7). In contrast to the bioregion ClaSSE, the top model for the elevation ClaSSE contained a different λ no shift parameter for low elevation ($\lambda_{L<L,L}$), mid elevation ($\lambda_{M<M,M}$), and high elevation ($\lambda_{H<H,H}$) taxa, but all extinction rates were constrained to be equal to one another (i.e., $\mu_L = \mu_M = \mu_H$). Posterior estimates for the three λ no shift parameters were significantly greater than the three λs associated with a state change (Fig. 4; Tables S11 and S12). The speciation rate associated with shifts between medium and high elevations ($\lambda_{M<M,H} = \lambda_{H<H,M}$; median = 13.11; 95% CI: 7.46–21.16) was significantly larger than speciation rates associated with shifts between low and medium elevations (median = 2.79; 95% CI: 1.05–5.69) and shifts between low and high elevations (median = 1.66; 95% CI: 0.29–4.55) (Fig. 4; Table S12). Finally, the single extinction

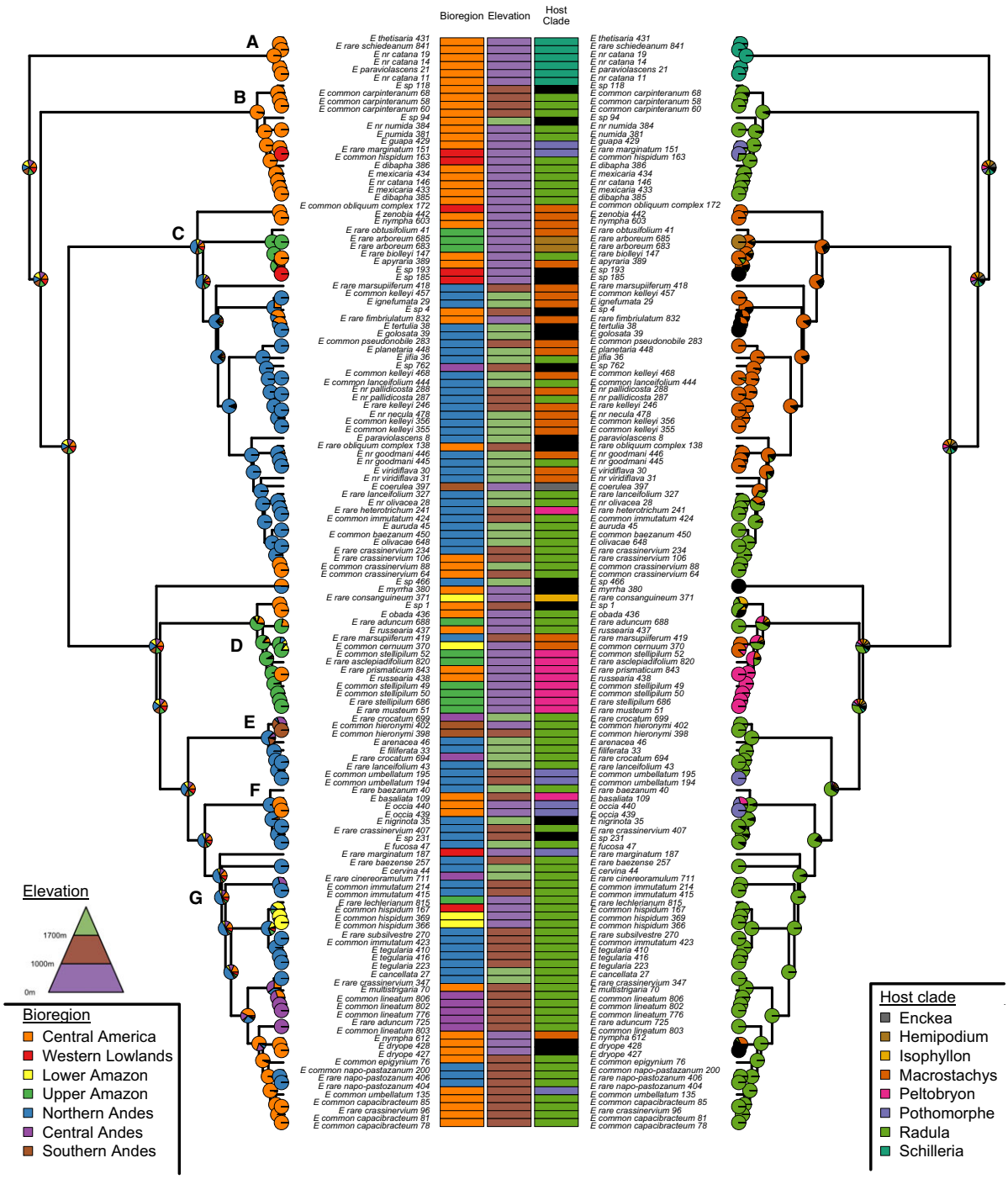

Figure 3. The distribution of bioregion, elevational, and host plant clade variation is displayed across the GBS tree. Individuals not identified to species are labeled as either rare or common (depending on how many individuals were collected), followed by the host plant species name. From left to right, the bars in the center of the figure display current tip states for bioregion, elevation, and host plant clade. Individuals without known host plant clade designations are colored black. Additional individual collection data can be found in Table S1. Groups of related *Eois* are labeled "A" — "G" for easy reference in the main text. Pie charts display the results of ancestral state reconstructions for bioregion (left side) and host plant clade (right side) for each node. See Fig. S6 for node support values and Fig. S7 for the ancestral trait reconstruction for elevation.

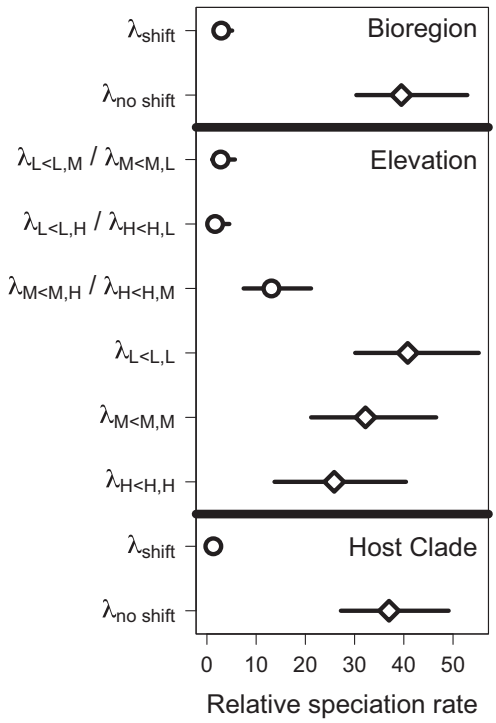

Figure 4. Posterior distributions of relative cladogenetic speciation rates (λ) associated with trait changes are depicted for each of the three ClaSSE models. All other parameter estimates can be found in Tables S9 (bioregion), S11 (elevation), and S13 (host plant clade). Each rate corresponds to an ancestor with one trait diverging into two descendants, one with the ancestral state and one with a derived trait. For example, the $\lambda_{L<L,M}$ rate corresponds to a low elevation ancestor diverging into one low elevation and one middle elevation descendant. The median of each posterior is denoted with a circle for λs associated with a trait shift or diamond for λs not associated with a trait shift, and the black bars correspond to 95% credible intervals. For the elevation ClaSSE, we found strong support for a symmetrical model where opposing speciation rates between a pair of states were equal to one another (e.g., $\lambda_{L<L,M} = \lambda_{M<M,L}$). For information on whether individual parameters were significantly different from one another, see Tables S10 (bioregion), S12 (elevation), and S14 (host plant clade). L, low elevation; M, mid elevation; H, high elevation.

rate (μ; median = 45.81; 95% CI: 34.13–59.80) was significantly larger than all of the λs in the model (Table S12).

For all 12 of the host plant clade ClaSSE alternative models, taxa were categorized as feeding on either Schilleria (Sc), Pothomorphe (Po), Peltobryon (Pe), Radula + Isophyllon (RI), Macrostachys + Hemipodium (MH), or unknown. Two of the three top models with Δ AIC < 2 constrained λs associated with a state change to be equal to one another. The top model of the host plant clade ClaSSE analysis constrained all λs not associated with a trait shift to be equal to one another but specified a different extinction rate for each host clade group (e.g., μ_{RI}). As in the bioregion ClaSSE, the posterior parameter estimate for λ no shift (median = 37.00; 95% CI: 27.22–49.11) was significantly greater than the estimate for λ shift (median = 1.30; 95% CI: 0.72–2.25) (Fig. 4; Tables S13 and S14). The extinction rates for Schilleria, Pothomorphe, and Peltobryon were similar in magnitude and significantly larger than the extinction rates for Radula + Isophyllon and Macrostachys + Hemipodium, which were similar in magnitude to each other (Tables S13 and S14).

Finally, we utilized BAMM to ask how many different macroevolutionary regimes existed across the evolutionary history of *Eois*. BAMM overwhelmingly supported a model with zero shifts in diversification rate across the GBS phylogeny (posterior parameter estimate = 0.977), as opposed to a model with one shift (posterior = 0.022) or two shifts (posterior < 0.001). Thus, the evolutionary history of *Eois* is consistent with the presence of a single macroevolutionary regime.

Discussion

Host conservatism, geography, and elevation all contributed substantively to the diversification of *Eois*, a genus of host specialized moths found throughout the Neotropics. We characterized these patterns of diversification by reconstructing four phylogenies using traditional Sanger sequencing methods (Figs. 2, S3) and a phylogeny using SNPs generated with a GBS approach (Fig. 3). Despite the relatively low number of SNPs we recovered (N = 4641; likely due to the high sequence divergence found across the genus; Wilson et al. 2012), the concordance in both topology and patterns of trait evolution indicates that GBS can be a useful alternative to more traditional sequencing methods as a source of phylogenetic data (e.g., Wagner et al. 2013; Ebel et al. 2015). For phylogenetic trees constructed from large SNP datasets, however, bioinformatic parameters and concatenation can negatively influence both topology and branch length estimation (Leaché et al. 2015a,b), potentially disrupting downstream comparative analyses. Namely, concatenation methods can be biased by gene flow, missing data, long-branch attraction, and poor taxon sampling relative to coalescent approaches (for a thorough review, see Liu et al. 2015), the latter being an especially important concern for this study given the high species diversity of *Eois*. Additionally, concatenation methods represent reduced models that contain fewer parameters than coalescent approaches, which can produce biased topologies that still have strong support values due to the small variance associated with a simpler model (Liu et al. 2015), though these effects can be at least partially mitigated by using concatenated sequences with invariant sites included (Leaché et al. 2015a), as we did here. Notwithstanding these potential issues, the similarity of results between the two sequencing methodologies we employed alleviates our concerns of how these potential biases might influence our understanding

of diversification in *Eois*. Hereafter, for simplicity, we primarily focus on the results from GBS.

Individuals clustered together according to three factors hypothesized to promote diversification in herbivorous insect lineages: host plant clade, bioregion, and elevation (Tables 1, 2; Figs. 3, S7). We employed broader geographic and elevational sampling distributions in our study relative to previous studies of *Eois* diversification (Strutzenberger et al. 2010; Wilson et al. 2012), which uncovered a complex phylogenetic hierarchy of trait evolution (e.g., Martiny et al. 2015). For example, many *Eois* groups have strong host conservatism (on species-rich clades of *Piper*) and weaker clustering for bioregion and elevation (e.g., group "G"; Figs. 3, S7), which supports a previous hypothesis that *Eois* diversification is characterized by small radiations of moths consuming plants within the same host clade and speciating along other axes of variation (Wilson et al. 2012). However, the relative strength of conservatism for host clade, elevation, and bioregion varied drastically among *Eois* groups (Figs. 3, S7). Despite this complexity, our findings support the hypothesis that the evolutionary history of *Eois* is characterized by relatively rare shifts to new host clades, bioregions, or elevational bands, followed by bouts of steady diversification along these new ecological axes (Figs. 3, S7).

The relative speciation rate associated with host plant clade shifts was small in magnitude compared to the rates not associated with host clade shifts (Fig. 4), likely because many host clade shifts occurred early in the diversification of *Eois* (Fig. 3). However, the host plant clade ClaSSE analysis yielded some evidence for elevated extinction rates associated with feeding on the Schilleria, Peltobryon, and Pothomorphe clades relative to the Radula + Isophyllon and Macrostachys + Hemipodium clades (~1.5 times larger; Tables S13 and S14). Macrostachys and Radula are the two most diverse Neotropical *Piper* lineages (~250 and 450 species, respectively; Martínez et al. 2015), and this high diversity might explain the reduced extinction rates for *Eois* lineages feeding on these clades. Finally, all of the individuals in the most basal *Eois* group ("A"; Figs. 2 and 3) feed on plants in the most basal Neotropical *Piper* clade Schilleria (Fig. 1), which is consistent with a pattern of codiversification between *Eois* and their hosts.

Despite the high number of geographic shifts among lineages, bioregion was significantly clustered for both datasets (Tables 1 and 2), suggesting that *Eois* lineages often diversify within ecologically defined bioregions (Fig. 1). The oldest *Eois* lineages are comprised mostly of individuals found in Panama (Group "A"; Fig. 3; Table S1), which is surprising given that most of Panama was thought to be submerged under the Central American Seaway (CAS) that divided North and South America until the middle Miocene (~13–15 Mya; Montes et al. 2015). It is possible that ancestral lineages of *Eois* dispersed into Panama following the closure of the CAS, or that the closure of the CAS was highly dynamic, with areas of present day Panama remaining above sea level and acting as refugia until the final closure. Evidence supporting the latter scenario (complex closure of the CAS) has been reported across a variety of organisms (Bacon et al. 2015). For example, a phylogenetic reconstruction of North and South American bees in the genus *Diadasia* supports a hypothesis of bee dispersal between the two continents approximately 15–20.5 Mya (Wilson et al. 2014). Geographic distributions among more apical *Eois* lineages did not support the role of the CAS as a recent barrier to dispersal; we instead found repeated shifts between Central and South America throughout the phylogeny (Fig. 3). The bioregion ClaSSE greatly favored a model with only two bioregions (Andean and non-Andean; Table S6). As in the host clade ClaSSE, relative speciation rates not associated with a shift between these bioregions were much larger than speciation rates associated with shifts (Fig. 4; Table S10). However, the bioregion ClaSSE found no support for differing extinction rates for Andean and non-Andean taxa (Table S6).

The distribution of elevational ranges across the *Eois* phylogeny supports a low-elevation origin of *Eois* in Central America, subsequent establishment in the high elevation Andean bioregion, and repeated colonization of low elevation non-Andean regions. This pattern is readily apparent in our phylogenetic trees (Figs. 3, S6), where the majority of basal individuals (Groups "A" and "B") occupy elevations below 1000 m. Previous molecular clock analyses suggest that much of the diversification in *Eois* coincided with increased Andean uplift, particularly during the Neogene (Strutzenberger and Fiedler 2011), which is consistent with our results. It is important to note, however, that the genus *Piper* also rapidly diversified during the rise of the Andes (Wilson et al. 2012), so uplift likely triggered accelerated *Eois* differentiation both directly through the genesis of novel habitats and indirectly by promoting host plant diversification. For *Eois* caterpillars, low and high elevations can be considered different ecological niches due to *Piper* species turnover across elevational bands and greater attack rates from natural enemies at low elevations (e.g., predatory ants or parasitoid flies and wasps; O'Donnell and Kumar 2006; Connahs et al. 2009; Rodríguez-Castañeda et al. 2011). As in the other two ClaSSE models, speciation rates not associated with shifts among elevational bands were much larger than rates associated with shifts (Fig. 4; Table S12). However, the speciation rate associated with shifts between middle and high elevations was significantly elevated compared to the other speciation rates associated with elevational shifts (Fig. 4; Table S12), supporting the hypothesis that Andean uplift was a strong driver of diversification for *Eois*.

Across all three ClaSSE analyses, speciation rates associated with a shift to a new trait state were much smaller in magnitude than speciation rates not associated with a shift (Fig. 4). However, this result does not mean that shifts to novel adaptive zones

were inconsequential for spurring *Eois* diversification. The patterns of trait evolution suggest that *Eois* lineages were continually exploring new ecological arenas across their evolutionary history, which occasionally resulted in speciation events associated with a trait shift along one trait axis, but not associated with trait shifts for other axes. It is likely that other adaptive zones not investigated here also played a role in driving *Eois* diversification. For example, *Piper* shows strong phytochemical variation between closely related species (Richards et al. 2015) and even within a single species (Glassmire et al. 2016). Thus, *Eois* could have diversified along phytochemical niche axes that were not quantified (Glassmire et al. 2016), which would also support the perspective that diversification in this group is driven by ecological opportunity associated with synergistic effects among multiple adaptive zones (Wilson et al. 2012). It is important to note that while we have found strong evidence for shifts in traits leading to diversification, the strong phylogenetic clustering of *Eois* with shared traits (Tables 1, 2) is also evidence for phylogenetic niche conservatism (Wiens 2004). It is likely that both shifts in adaptive zones and persistent diversification within zones (reflected in conservatism) are important in driving diversification in *Eois*. Further progress in this area will await future studies with greater trait resolution, such as analyzing the evolution of host associations at the species level.

Consistent with the influence of many drivers of diversification, the results from BAMM supported a model in which the overall diversification rate remained the same across the evolutionary history of *Eois*, suggesting that no particular colonization of a novel adaptive zone yielded an exceptional burst of diversification. The great diversity of this genus is perhaps best explained by a slow and steady exploration of ecological niche space across multiple axes of variation, producing complex hierarchical patterns. Oftentimes, macroevolutionary studies have focused on understanding how a single driver can spur diversification; however, many taxonomic groups, including *Eois*, have multiplied in response to a suite of interconnected factors (Voje et al. 2015). As such, future studies examining diversification in herbivorous insects should account for geographic and elevational distributions in addition to patterns of host use, especially for groups occurring in regions with complex geological histories.

AUTHORS CONTRIBUTION

A.M.S., L.A.D., and M.L.F. developed the original idea for this research and secured funding. A.E.G., A.M.S., E.J.T., J.P.J., J.S.M., L.A.D., L.A.R., M.A.Q.-A., and T.R.W. contributed to the collection of samples from across the Neotropics. E.J.T. and M.A.Q.-A. identified the *Piper* specimens, while J.S.M. and L.A.D. identified the *Eois* specimens. J.P.J., J.S.W., and M.L.F. extracted DNA and analyzed the Sanger dataset. J.P.J. and T.L.P. constructed the libraries for Illumina sequencing and analyzed the GBS dataset. J.P.J. wrote the initial draft and all authors contributed in revising the manuscript.

ACKNOWLEDGMENTS

This research was largely funded through grants from the National Science Foundation (DEB-1145609 and DEB-1442103), and partially by a Trevor James McMinn professorship to M.L.F. We thank: Luis Alberto Salagaje, Heidi Connahs, Humberto Garcia Lopez, Harold Greeney, Patrick Melarkey, Genoveva Rodríguez-Castañeda, Wilmer Rosendo Simbaña, Gerardo Vega Chavarria, and several Earthwatch volunteers for field collections and logistical support; Kris Kruse and Craig Osborne from the Nevada Genomics Center and Angela Hornsby for providing invaluable assistance with DNA sequencing; Jim Fordyce for imparting his statistical wizardry; Chris Feldman, Elizabeth Leger, Steve Vander Wall, and the University of Nevada, Reno EECB peer review group for providing valuable comments on early versions of the manuscript; and Associate Editor Jessica Light, Fabien Condamine, and three anonymous reviewers for providing valuable comments that improved later versions of the manuscript.

DATA ARCHIVING

The doi for our data is https://doi.org/10.5061/dryad.k0gq6.

LITERATURE CITED

Arenas, M. 2015. Trends in substitution models of molecular evolution. Front. Genet. 6:319.

Bacon, C. D., D. Silvestro, C. Jaramillo, B. T. Smith, P. Chakrabarty, and A. Antonelli. 2015. Biological evidence supports an early and complex emergence of the Isthmus of Panama. Proc. Natl. Acad. Sci. USA 112:6110–6115.

Bagley, J. C., and J. B. Johnson. 2014. Phylogeography and biogeography of the lower Central American Neotropics: diversification between two continents and between two seas. Biol. Rev. 89:767–790.

Becerra, J. X. 1999. Macroevolution of insect-plant associations: the relevance of host biogeography to host affiliation. Proc. Natl. Acad. Sci. USA 96:12626–12631.

Benkman, C. W. 1993. Adaptation to single resources and the evolution of crossbill (*Loxia*) diversity. Ecol. Monogr. 63:305–325.

Benkman, C. W., T. L. Parchman, and E. T. Mezquida. 2010. Patterns of coevolution in the adaptive radiation of crossbills. Ann. NY Acad. Sci. 1206:1–16.

Blomberg, S. P., and T. Garland. 2002. Tempo and mode in evolution: phylogenetic inertia, adaptation and comparative methods. J. Evol. Biol. 15:899–910.

Blomberg, S. P., T. Garland, and A. R. Ives. 2003. Testing for phylogenetic signal in comparative data: behavioral traits are more labile. Evolution 57:717–745.

Brehm, G., F. Bodner, P. Strutzenberger, F. Hünefeld, and K. Fiedler. 2011. Neotropical *Eois* (Lepidoptera: Geometridae): checklist, biogeography, diversity, and description patterns. Ann. Entomol. Soc. Am. 104:1091–1107.

Brehm, G., P. D. N. Hebert, R. K. Colwell, M.-O. Adams, F. Bodner, K. Friedemann, L. Möckel, K. Fiedler. 2016. Turning up the heat on a hotspot: DNA barcodes reveal 80% more species of geometrid moths along an Andean elevational gradient. PLoS ONE 11:e0150327.

Burns, J. M., D. H. Janzen, M. Hajibabaei, W. Hallwachs, and P. D. N. Hebert. 2008. DNA barcodes and cryptic species of skipper butterflies in the genus *Perichares* in Area de Conservación Guanacaste, Costa Rica. Proc. Natl. Acad. Sci. USA 105:6350–6355.

Carlquist, S. 1974. Island biology. Columbia Univ. Press, New York.

Calatayud, J., J. L. Hórreo, J. Madrigal-González, A. Migeon, M. A. Rodríguez, S. Magalhães, and J. Hortal. 2016. Geography and major

host evolutionary transitions shape the resource use of plant parasites. Proc. Natl. Acad. Sci. USA 113:9840–9845.

Chazot, N., K. R. Willmott, F. L. Condamine, D. L. De-Silva, A. V. L. Freitas, G. Lamas, H. Morlon, C. E. Giraldo, C. D. Jiggins, M. Joron, et al. 2016. Into the Andes: multiple independent colonizations drive montane diversity in the Neotropical clearwing butterflies Godyridina. Mol. Ecol. 25:5765–5784.

Condamine, F. L., F. A. H. Sperling, N. Wahlberg, J. Y. Rasplus, and G. J. Kergoat. 2012. What causes latitudinal gradients in species diversity? Evolutionary processes and ecological constraints on swallowtail biodiversity. Ecol. Lett. 15:267–277.

Connahs, H., G. Rodríguez-Castañeda, T. Walters, T. Walla, and L. Dyer. 2009. Geographic variation in host-specificity and parasitoid pressure of an herbivore (Geometridae) associated with the tropical genus *Piper* (Piperaceae). J. Insect Sci. 9:28.

Darriba, D., G. L. Taboada, R. Doallo, and D. Posada. 2012. jModelTest 2: more models, new heuristics and parallel computing. Nat. Methods 9:772.

Daza, J. M., T. A. Castoe, and C. L. Parkinson. 2010. Using regional comparative phylogeographic data from snake lineages to infer historical processes in Middle America. Ecography 33:343–354.

Dyer, L. A., M. S. Singer, J. T. Lill, J. O. Stireman, G. L. Gentry, R. J. Marquis, R. E. Ricklefs, H. F. Greeney, D. L. Wagner, H. C. Morais, et al. 2007. Host specificity of Lepidoptera in tropical and temperate forests. Nature 448:696–699.

Dyer, L. A., T. R. Walla, H. F. Greeney, J. O. Stireman, and R. F. Hazen. 2010. Diversity of interactions: a metric for studies of biodiversity. Biotropica 42:281–289.

Eaton, D. A. R. 2014. PyRAD: assembly of de novo RADseq loci for phylogenetic analyses. Bioinformatics 30:1844–1849.

Ebel, E. R., J. M. DaCosta, M. D. Sorenson, R. I. Hill, A. D. Briscoe, K. R. Willmott, and S. P. Mullen. 2015. Rapid diversification associated with ecological specialization in Neotropical *Adelpha* butterflies. Mol. Ecol. 24:2392–2405.

Edgar, R. C. 2004. MUSCLE: multiple sequence alignment with high accuracy and high throughput. Nucleic Acids Res. 32:1792–1797.

Edger, P. P., H. M. Heidel-Fischer, M. Bekaert, J. Rota, G. Glöckner, A. E. Platts, D. G. Heckel, J. P. Der, E. K. Wafula, M. Tang, et al. 2015. The butterfly plant arms-race escalated by gene and genome duplications. Proc. Natl. Acad. Sci. USA 112:8362–8366.

Ehrlich, P. R., and P. H. Raven. 1964. Butterflies and plants: a study in coevolution. Evolution 18:586–608.

Esquerré, D., and J. S. Keogh. 2016. Parallel selective pressures drive convergent diversification of phenotypes in pythons and boas. Ecol. Lett. 19:800–809.

FitzJohn, R. G. 2012. Diversitree: comparative phylogenetic analyses of diversification in R. Methods Ecol. Evol. 3:1084–1092.

Fordyce, J. A. 2010. Host shifts and evolutionary radiations of butterflies. Proc. R Soc. B 277:3735–3743.

Forister, M. L., V. Novotny, A. K. Panorska, L. Baje, Y. Basset, P. T. Butterill, L. Cizek, P. D. Coley, F. Dem, I. R. Diniz, et al. 2015. The global distribution of diet breadth in insect herbivores. Proc. Natl. Acad. Sci. USA 112:442–447.

Gentry, G. L., and L. A. Dyer. 2002. On the conditional nature of Neotropical caterpillar defenses against their natural enemies. Ecology 83:3108–3119.

Givnish, T. J., K. C. Millam, A. R. Mast, T. B. Paterson, T. J. Theim, A. L. Hipp, J. M. Henss, J. F. Smith, K. R. Wood, and K. J. Sytsma. 2009. Origin, adaptive radiation and diversification of the Hawaiian lobeliads (Asterales: Campanulaceae). Proc. R. Soc. B 276:407–416.

Glassmire, A. E., C. S. Jeffrey, M. L. Forister, T. L. Parchman, C. C. Nice, J. P. Jahner, J. S. Wilson, T. R. Walla, L. A. Richards, A. M. Smilanich, et al. 2016. Intraspecific phytochemical variation shapes community and population structure for specialist caterpillars. New Phytol. 212:208–219.

Goldberg, E. E., and B. Igić. 2012. Tempo and mode in plant breeding system evolution. Evolution 66:3701–3709.

Haines, W. P., P. Schmitz, and D. Rubinoff. 2014. Ancient diversification of *Hyposmocoma* moths in Hawaii. Nat. Commun. 5:3502.

Hebert, P. D. N., E. H. Penton, J. M. Burns, D. H. Janzen, and W. Hallwachs. 2004. Ten species in one: DNA barcoding reveals cryptic species in the Neotropical skipper butterfly *Astraptes fulgerator*. Proc. Natl. Acad. Sci. USA 101:14812–14817.

Hodges, S. A., and M. L. Arnold. 1995. Spurring plant diversification: are floral nectar spurs a key innovation? Proc. R Soc. B 262:343–348.

Hoorn, C., F. P. Wesselingh, H. ter Steege, M. A. Bermudez, A. Mora, J. Sevink, I. Sanmartín, A. Sanchez-Meseguer, C. L. Anderson, J. P. Figueiredo, et al. 2010. Amazonia through time: Andean uplift, climate change, landscape evolution, and biodiversity. Science 330:927–931.

Janz, N. 2011. Ehrlich and Raven revisited: mechanisms underlying codiversification of plants and enemies. Annu. Rev. Ecol. Evol. Syst. 42:71–89.

Janzen, D. H., W. Hallwachs, P. Blandin, J. M. Burns, J. M. Cadiou, I. Chacón, T. Dapkey, A. R. Deans, M. E. Epstein, B. Espinoza, et al. 2009. Integration of DNA barcoding into an ongoing inventory of complex tropical biodiversity. Mol. Ecol. Res. 9 (Suppl.):1–26.

Jaramillo, M. A., R. Callejas, C. Davidson, J. F. Smith, A. C. Stevens, and E. J. Tepe. 2008. A phylogeny of the tropical genus Piper using ITS and the chloroplast intron psbJ-petA. Syst. Bot. 33:647–660.

Kamilar, J. M., and N. Cooper. 2013. Phylogenetic signal in primate behavior, ecology and life history. Phil. Trans R. Soc. B 368:20120341.

Lack, D. 1947. Darwin's finches. Cambridge Univ. Press, Cambridge.

Lagomarsino, L. P., F. L. Condamine, A. Antonelli, A. Mulch, and C. C. Davis. 2016. The abiotic and biotic drivers of rapid diversification in Andean bellflowers (Campanulaceae). New Phytol. 210:1430–1442.

Lanfear, R., P. B. Frandsen, A. M. Wright, T. Senfeld, and B. Calcott. 2017. PartitionFinder 2: new methods for selecting partitioned models of evolution for molecular and morphological phylogenetic analyses. Mol. Biol. Evol. 34:772–773.

Langmead, B., and S. L. Salzberg. 2012. Fast gapped-read alignment with Bowtie 2. Nat. Methods 9:357–359.

Leaché, A. D., and J. R. Oaks. 2017. The utility of single nucleotide polymorphism (SNP) data in phylogenetics. Annu. Rev. Ecol. Evol. Syst. 48:69–84.

Leaché, A. D., B. L. Banbury, J. Felsenstein, A. Nieto-Montez de Oca, and A. Stamatakis. 2015a. Short tree, long tree, right tree, wrong tree: new acquisition bias corrections for inferring SNP phylogenies. Syst. Biol. 64:1032–1047.

Leaché, A. D., A. S. Chavez, L. N. Jones, J. A. Grummer, A. D. Gottscho, and C. W. Linkem. 2015b. Phylogenomics of phrynosomatid lizards: conflicting signals from sequence capture versus restriction site associated DNA sequencing. Genome Biol. Evol. 7:706–719.

Lerner, H. R. L., M. Meyer, H. F. James, M. Hofreiter, and R. C. Fleischer. 2011. Multilocus resolution of phylogeny and timescale in the extant adaptive radiation of Hawaiian honeycreepers. Curr. Biol. 21:1838–1844.

Li, H., B. Handsaker, A. Wysoker, T. Fennell, J. Ruan, N. Homer, G. Marth, G. Abecasis, R. Durbin, and 1000 Genome Project Data Processing Subgroup. 2009. The sequence alignment/map format and SAMtools. Bioinformatics 25:2078–2079.

Liu, L., Z. Xi, S. Wu, C. C. Davis, and S. V. Edwards. 2015. Estimating phylogenetic trees from genome-scale data. Ann. NY Acad. Sci. 1360:36–53.

Losos, J. B. 2010. Adaptive radiation, ecological opportunity, and evolutionary determinism. Am. Nat. 175:623–639.

Mahler, D. L., T. Ingram, L. J. Revell, and J. B. Losos. 2013. Exceptional convergence on the macroevolutionary landscape in island lizard radiations. Science 341:292–295.

Martin, C. H., and Wainwright, P. C. 2011. Trophic novelty is linked to exceptional rates of morphological diversification in two adaptive radiations of Cyprinodon pupfish. Evolution 65:2197–2212.

Martínez, C., M. R. Carvalho, S. Madriñán, and C. A. Jaramillo. 2015. A late Cretaceous *Piper* (Piperaceae) from Colombia and diversification patterns for the genus. Am. J. Bot. 102:273–289.

Martiny, J. B. H., S. E. Jones, J. T. Lennon and A. C. Martiny. 2015. Microbiomes in light of traits: a phylogenetic perspective. Science 350:aac9323.

Matschiner, M., R. Hanel, and W. Salzburger. 2011. On the origin and trigger of the notothenioid adaptive radiation. PLoS ONE 6:e18911.

Mitter, C., B. Farrell, and B. Wiegmann. 1988. The phylogenetic study of adaptive zones: has phytophagy promoted insect diversification? Am. Nat. 132:107–128.

Montes, C., A. Cardona, C. Jaramillo, A. Pardo, J. C. Silva, V. Valencia, C. Ayala, L. C. Pérez-Angel, L. A. Rodriguez-Parra, V. Ramirez, et al. 2015. Middle Miocene closure of the Central American Seaway. Science 348:226–229.

Muschick, M., A. Indermaur, and W. Salzburger. 2012. Convergent evolution within an adaptive radiation of cichlid fishes. Curr. Biol. 22:2362–2368.

O'Donnell, S., and Kumar, A. 2006. Microclimatic factors associated with elevational changes in army ant density in tropical montane forest. Ecol. Entomol. 31:491–498.

Ohio Supercomputer Center. 1987. Ohio Supercomputer Center. Columbus OH: Ohio Supercomputer Center. http://osc.edu/ark:/19495/f5s1ph73.

Pagel, M. 1994. Detecting correlated evolution on phylogenies: a general method for the comparative analysis of discrete characters. Proc. R Soc. B 255:37–45.

———. 1999. Inferring the historical patterns of biological evolution. Nature 401:877–884.

Paradis, E., J. Claude, and K. Strimmer. 2004. APE: analyses of phylogenetics and evolution in R language. Bioinformatics 20:289–290.

Parchman, T. L., Z. Gompert, J. Mudge, F. D. Schilkey, C. W. Benkman and C. A. Buerkle. 2012. Genome-wide association genetics of an adaptive trait in lodgepole pine. Mol. Ecol. 21:2991–3005.

Parker, J., A. Rambaut, and O. G. Pybus. 2008. Correlating viral phenotypes with phylogeny: accounting for phylogenetic uncertainty. Infect. Genet. Evol. 8:239–246.

Price, M. N., P. S. Dehal, and A. P. Arkin. 2010. FastTree 2–approximately maximum-likelihood trees for large alignments. PLoS ONE 5:e9490.

Puritz, J. B., C. M. Hollenbeck, and J. R. Gold. 2014. dDocent: a RADseq, variant-calling pipeline designed for population genomics of non-model organisms. PeerJ 2:e431.

Quijano-Abril, M. A., R. Callejas-Posada and D. R. Miranda-Esquivel. 2006. Areas of endemism and distribution patterns for Neotropical *Piper* species (Piperaceae). J. Biogeogr. 33:1266–1278.

R Core Team. 2015. R: a language and environment for statistical computing. R Foundation for Statistical Computing, Vienna, Austria. URL http://www.R-project.org/

Rabosky, D. L. 2014. Automatic detection of key innovations, rate shifts, and diversity dependence on phylogenetic trees. PLoS ONE 9:e89543.

Rabosky, D. L., M. Grundler, C. Anderson, P. Title, J. J. Shi, J. W. Brown, H. Huang, and J. G. Larson. 2014. BAMMtools: an R package for the analysis of evolutionary dynamics on phylogenetic trees. Methods Ecol. Evol. 5:701–707.

Revell, L. J. 2012. phytools: an R package for phylogenetic comparative biology (and other things). Methods Ecol. Evol. 3:217–223.

Richards, L. A., L. A. Dyer, M. L. Forister, A. M. Smilanich, C. D. Dodson, M. D. Leonard, and C. S. Jeffrey. 2015. Phytochemical diversity drives plant-insect community diversity. Proc. Natl. Acad. Sci. USA 112:10973–10978.

Rodríguez-Castañeda, G., L. A. Dyer, G. Brehm, H. Connahs, R. E. Forkner, and T. R. Walla. 2010. Tropical forests are not flat: how mountains affect herbivore diversity. Ecol. Lett. 13:1348–1357.

Rodríguez-Castañeda, G., R. E. Forkner, E. J. Tepe, G. L. Gentry, and L. A. Dyer. 2011. Weighing defensive and nutritive roles of ant mutualists across a tropical altitudinal gradient. Biotropica 43:343–350.

Rognes, T., T. Flouri, B. Nichols, C. Quince, and F. Mahé. 2016. VSEARCH: a versatile open source tool for metagenomics. PeerJ 4:e2584.

Ronquist, F., M. Teslenko, P. van der Mark, D. L. Ayres, A. Darling, S. Höhna, B. Larget, L. Liu, M. A. Suchard, and J. P. Huelsenbeck. 2012. MrBayes 3.2: efficient Bayesian phylogenetic inference and model choice across a large model space. Syst. Biol. 61:539–542.

Schluter, D. 2000. The ecology of adaptive radiation. Oxford Univ. Press, Oxford.

Seifert, C. L., F. Bodner, G. Brehm, and K. Fiedler. 2015. Host plant associations and parasitism of south Ecuadorian *Eois* species (Lepidoptera: Geometridae) feeding on *Peperomia* (Piperaceae). J. Insect Sci. 15: 119.

Shimodaira, H., and M. Hasegawa. 1999. Multiple comparisons of log-likelihoods with applications to phylogenetic inference. Mol. Biol. Evol. 16:1114–1116.

Sihvonen, P., M. Mutanen, L. Kaila, G. Brehm, A. Hausmann, and H. S. Staude. 2011. Comprehensive molecular sampling yields a robust phylogeny for geometrid moths (Lepidoptera: Geometridae). PLoS ONE 6:e20356.

Simpson, G. G. 1953. The major features of evolution. Columbia Univ. Press, New York.

Slatkin, M., and Maddison, W. P. 1989. A cladistics measure of gene flow inferred from the phylogenies of alleles. Genetics 123:603–613.

Stroud, J. T., and J. B. Losos. 2016. Ecological opportunity and adaptive radiation. Annu. Rev. Ecol. Evol. Syst. 47:507–532.

Strutzenberger, P., and K. Fiedler. 2011. Temporal patterns of diversification in Andean *Eois*, a species-rich clade of moths (Lepidoptera, Geometridae). J. Evol. Biol. 24:919–925.

Strutzenberger, P., G. Brehm, F. Bodner, and K. Fiedler 2010. Molecular phylogeny of *Eois* (Lepidoptera, Geometridae): evolution of wing patterns and host plant use in a species-rich group of Neotropical moths. Zool. Scr. 39:603–620.

Strutzenberger, P., G. Brehm, and K. Fiedler. 2011. DNA barcoding-based species delimitation increases species count of *Eois* (Geometridae) moths in a well-studied tropical mountain forest by up to 50%. Insect Sci. 18:349–362.

Turchetto-Zolet, A. C., F. Pinheiro, F. Salgueiro, and C. Palma-Silva. 2013. Phylogeographical patterns shed light on evolutionary processes in South America. Mol. Ecol. 22:1193–1213.

Voje, K. L., H. H. Øistein, L. H. Liow, and N. C. Stenseth. 2015. The role of biotic forces in driving macroevolution: beyond the Red Queen. Proc. R. Soc. B 282:20150186.

Wagner, C. E., I. Keller, S. Wittwer, O. M. Selz, S. Mwaiko, L. Greuter, A. Sivasundar, and O. Seehausen. 2013. Genome-wide RAD sequence data provide unprecedented resolution of species boundaries and relationships in the Lake Victoria cichlid adaptive radiation. Mol. Ecol. 22:787–798.

Wang, T. H., Y. K. Donaldson, R. P. Brettle, J. E. Bell, and P. Simmonds. 2001. Identification of shared populations of Human Immunodeficiency Virus

Type 1 infecting microglia and tissue macrophages outside the central nervous system. J. Virol. 75:11686–11699.

Wheat, C. W., H. Vogel, U. Wittstock, M. F. Braby, D. Underwood, and T. Mitchell-Olds. 2007. The genetic basis of a plant-insect coevolutionary key innovation. Proc. Natl. Acad. Sci. USA 104:20427–20431.

Wiens, J. J. 2004. Speciation and ecology revisited: phylogenetic niche conservatism and the origin of species. Evolution 58:193–197.

Wilson, J. S., M. L. Forister, L. A. Dyer, J. M. O'Connor, K. Burls, C. R. Feldman, M. A. Jaramillo, J. S. Miller, G. Rodríguez-Castañeda, E. J. Tepe, et al. 2012. Host conservatism, host shifts and diversification across three trophic levels in two Neotropical forests. J. Evol. Biol. 25:532–546.

Wilson, J. S., O. M. Carril, and S. D. Sipes. 2014. Revisiting the Great American Biotic Interchange through analyses of amphitropical bees. Ecography 37:791–796.

Wilson, J. S., J. P. Jahner, M. L. Forister, E. S. Sheehan, K. A. Williams, and J. P. Pitts. 2015. North American velvet ants form one of the world's largest known Müllerian mimicry complexes. Curr. Biol. 25:R704–R706.

Winkler, I. S., and C. Mitter. 2008. The phylogenetic dimension of insect-plant interactions: a review of recent evidence. Pp. 203–215 *in* K. J. Tilmon, ed. Specialization, speciation, and radiation: the evolutionary biology of herbivorous insects. California Univ. Press, Berkeley, CA.

Yoder, J. B., E. Clancey, S. des Roches, J. M. Eastman, L. Gentry, W. Godsoe, T. J. Hagey, D. Jochimsen, B. P. Oswald, J. Robertson, et al. 2010. Ecological opportunity and the origin of adaptive radiations. J. Evol. Biol. 23:1581–1596.

Associate Editor: J. Light

Supporting Information

Additional Supporting Information may be found in the online version of this article at the publisher's website:

Table S1. Collection data for each *Eois* individual included in this study, including collection locality, collection country, elevation, host plant species, and host plant clade.

Table S2. PCR primers for each gene are listed. Wingless and EF1-alpha primers have universal sequencing primers attached on the ends to facilitate sequencing.

Table S3. Summary of PCR protocols and master mix recipe for the three genes sequenced in this study.

Table S4. Summary of model comparison results for the ancestral state reconstruction of elevation as a categorical trait using the Sanger dataset. For each model, the number of parameters (*N*), log-likelihood, AIC, and Δ AIC are listed.

Table S5. Summary of model comparison results for the ancestral state reconstruction of elevation as a categorical trait using the GBS dataset.

Table S6. Model selection results for the bioregion ClaSSE model. We evaluated 32 alternative models with maximum likelihood and parameterized the top model (based on AIC) with MCMC.

Table S7. Model selection results for the elevation ClaSSE model. We evaluated 24 alternative models with maximum likelihood and parameterized the top model (based on AIC) with MCMC.

Table S8. Model selection results for the host clade ClaSSE model.

Table S9. Posterior parameter estimates of speciation rates (λ) and extinction rates (μ) from the bioregion ClaSSE model. In the model, $\lambda_{A<A,N}$ and $\lambda_{N<N,A}$ were constrained to be equal to one another (λ shift), $\lambda_{A<A,A}$ and $\lambda_{N<N,N}$ were constrained to be equal to one another (λ no shift), and μ_A and μ_N were constrained to be equal to one another (μ). A = Andean; N = Non-Andean.

Table S10. For each pairwise combination of parameters in the bioregion ClaSSE model, the joint probability (P_J) was calculated to determine if posterior distributions were significantly different from one another.

Table S11. Posterior parameter estimates of speciation rates (λ) and extinction rates (μ) from the elevation ClaSSE model.

Table S12. For each pairwise combination of parameters in the elevation ClaSSE model, the joint probability (P_J) was calculated to determine if posterior distributions were significantly different from one another.

Table S13. Posterior parameter estimates of speciation rates (λ) and extinction rates (μ) from the host clade ClaSSE model.

Table S14. For each pairwise combination of parameters in the host clade ClaSSE model, the joint probability (P_J) was calculated to determine if posterior distributions were significantly different from one another.

Fig. S1. A histogram display the distribution of *Eois* individuals included in Sanger sequencing collected across elevation.

Fig. S2. A histogram display the distribution of *Eois* individuals included in GBS sequencing collected across elevation.

Fig. S3. The evolutionary relationships of 107 *Eois* were reconstructed using one mitochondrial gene (COI) and two nuclear genes (EF1-α; WG).

Fig. S4. The distribution of bioregion, elevational, and host clade variation is displayed across the concatenated Sanger phylogeny (COI; EF1-α; WG).

Fig. S5. The distribution of bioregion, elevational, and host clade variation is displayed across the concatenated Sanger phylogeny (COI; EF1-α; WG).

Fig. S6. The topology of the GBS maximum-likelihood phylogeny is displayed. Individuals not identified to species are labeled as either rare or common (depending on how many individuals were collected), followed by the host plant species name.

Fig. S7. The distribution of bioregion, elevational, and host clade variation is displayed across the GBS tree. Individuals not identified to species are labeled as either rare or common (depending on how many individuals were collected), followed by the host plant species name.